Anal Bioanal Chem (2017) 409:431–438
DOI 10.1007/s00216-016-9796-1

RESEARCH PAPER

A novel carbon material with nanopores prepared using a metal–organic framework as precursor for highly selective enrichment of N-linked glycans

Yanan Wang[1] · **Jiaxi Wang**[1] · **Mingxia Gao**[1] · **Xiangmin Zhang**[1]

Received: 13 April 2016 / Revised: 7 July 2016 / Accepted: 14 July 2016 / Published online: 2 August 2016

Abstract Protein glycosylation plays a key role in many biological processes. In this study, a novel carbon material with nanopores was prepared by carbonization of metal–organic framework (MOF) Mil-101(Cr). The parent MOF assembled from metal ions with bridging organic linkers had many fascinating properties, such as ultrahigh surface area, suitable nanopore structure, and especially a large amount of carbon after being calcined. Due to the strong interactions between carbon and glycans as well as the size-exclusion effect of pore against protein, the N-linked glycans from standard glycoprotein or complex human serum proteins could be identified with high efficiency. The simple synthesis method as well as good enrichment efficiency made this novel carbon material a promising tool for glycosylation research.

Keywords Protein glycosylation · Carbon material · Nanopores · MOF · Enrichment · N-linked glycans

Introduction

Protein glycosylation is one of the most important post-translational modifications of proteins, it plays an essential role in biological processes [1–4]. Generally, protein glycosylation includes two main categories: the glycans of N-linked glycosylation and the glycans of O-glycosylation. The N-glycans are conjugated to proteins through asparagine residues consisting of a consensus tripeptide sequence of Asn-X-Ser/Thr (X can be any amino acid except proline) and the O-glycans which are linked to serine or threonine residues [5]. At present, most studies are focused on the N-glycans because their configuration is closely related to various diseases [6–8]. In recent years, mass spectrometry (MS) as a key technology has been applied to glycoprotein analysis. However, due to the poor ionization efficiency and low abundance of glycans, the MS detection becomes extremely difficult. Therefore, it is highly desirable to design novel enrichment materials for the selective isolation of glycans digested from proteins [9–12].

So far some methods and materials for glycan enrichment have been developed. Graphite affinity column and hydrophilic interaction liquid chromatography (HILIC), which relies on the physical interactions between glycans and the stationary phase, are the most widely used enrichment methods [13–16]. However, they always suffer from the low specificity for the reason of simultaneously capturing nonglycans. Though lectin-based enrichment offers improved specificity, different types of lectins show diverse affinities for various glycans; thus for complex samples, it is necessary to combine different types of lectins. Based on the hydrophobic and polar interactions between carbon and glycans, active carbon material has been reported to be a promising material in enrichment of glycans [17, 18]. However, because of the restrictions on macroporous structure, complex proteins are still adsorbed due to the weak size-exclusion ability [19].

Metal–organic frameworks (MOFs) are a new class of porous solid materials with some special properties, such as high surface area and permanent porosity [20, 21]. In the recent researches for MOFs, many of them have been utilized in

Published in the topical collection *Glycomics, Glycoproteomics and Allied Topics* with guest editors Yehia Mechref and David Muddiman.

Electronic supplementary material The online version of this article (doi:10.1007/s00216-016-9796-1) contains supplementary material, which is available to authorized users.

✉ Mingxia Gao
mxgao@fudan.edu.cn

[1] Department of Chemistry and Institute of Biomedical Sciences, Fudan University, Shanghai 200433, China

gas adsorption, catalysis, drug delivery, and separation with the advantages of high surface area, uniformly structured cavities, and available modification [22–24]. Also, MOFs have stimulated increasing research interest in analytical chemistry [25] and more and more MOFs have been employed in proteomics such as the enrichment of low-abundance peptides [25, 26] and study of phosphoproteome [26–30].

Since the first report on MOFs-derived nanoporous carbon materials by Xu et al. [31], several types of carbon materials have been prepared by carbonization of MOFs [32, 33]. Compared with other mesoporous carbon materials for glycan enrichment [5, 34, 35], MOF-prepared nanoporous carbon materials keep high surface area and high carbon contents, especially the more suitable nanopore structure. All of these make this material present a better effect in size-exclusion of proteins for glycans.

Mil-101(Cr) is an excellent MOF as the template material because of its extra high specific surface area and pore volume. In addition, it has moisture and acid-resistant stability and thermal stability when temperature is higher than 200 °C [36, 37]. Therefore, after simple hydrothermal reaction and carbonization under a high temperature, we obtained a novel carbon material consisting of high surface area and suitable nanopore structure. And for the first time, it was used in the enrichment of N-linked glycans. It has several advantages as the enrichment material. Firstly, the large specific surface area provided a wide place for the distribution of carbon, which made this material have high sample loading capability and strong interaction toward glycan molecules. Furthermore, the suitable nanopore structure made this material present a better effect in size-exclusion of proteins for glycans. Based on these unique properties, the carbonized Mil-101 displayed high efficiency in enriching N-linked glycans from complex biosamples.

Materials and methods

Materials

2,5-Dihydroxy-benzoic acid (DHB), chicken egg albumin (OVA), and bovine serum albumin (BSA) were purchased from Sigma-Aldrich (St, Louis, MO, USA), and peptide-N-glycosidase (PNGase F) was from New England Biolabs. The ultrapure water used in the experiment was prepared by the Milli-Q system (Millipore, Bedford, MA). Acetonitrile (ACN) and trifluoroacetic acid (TFA) were purchased from Merck (Darmstadt, Germany). Human serum was supplied by the Zhongshan Hospital. Chromic nitrate nonahydrate ($Cr(NO_3)_3{\cdot}9H_2O$), terephthalic acid (H_2BDC), fluorhydric acid, chromic oxide (Cr_2O_3), and other reagents were obtained from Sinopharm Group Co. Ltd.

Preparation of Mil-101(Cr) crystals

$Cr(NO_3)_3{\cdot}9H_2O$ (2 g) and terephthalic acid (H_2BDC) (820 mg) were dispersed in ultrapure water (24 mL), then 2 mL fluorhydric acid was added dropwise into the dispersion solution. At last, the suspension was heated under autogenous pressure in a Teflon-lined stainless steel autoclave at 220 °C for 8 h [37]. The green powder of Mil-101 was collected by centrifugation, then washed several times with ethanol, and dried at 50 °C in vacuum oven.

Carbonization of Mil-101(Cr)

The dried Mil-101 was under a N_2 flow at 800 °C for 2 h, with a heating rate of 10 °C min^{-1}. After that, the obtained carbonized Mil-101(Cr) was stored for the further use.

Characterization

Transmission electron microscopy (TEM) images were taken with a JEOL2011 microscope (Japan) operating at 200 kV. Field scanning electron microscopy (SEM) images was acquired on a Nova NanoSem 450. Powder X-ray diffraction patterns were recorded on a Bruker D4 X-ray diffractometer with Ni-filtered Cu Kαradiation (40 kV, 40 mA). The Brunauer-Emmett-Teller (BET) method was utilized to calculate the specific surface areas (SBET) using adsorption data in a relative pressure range from 0.011 to 0.98. By using the Density Functional Theory (DFT) method, the pore volumes and pore size distributions were derived from the desorption branches of the isotherms. The Raman spectra were recorded at room temperature on a LabRam-1B Raman spectrometer with a laser at an excitation wavelength of 632.8 nm.

Selective enrichment of N-linked glycans from standard peptides and human serum with carbonized Mil-101(Cr)

At first, the N-linked glycans which were digested from chicken ovalbumin (OVA) were chosen to investigate the enrichment ability. The detailed experiment process was listed in the Electronic Supplementary Material (ESM). And then carbonized Mil-101(Cr) (10 mg) was suspended in 1 mL of ultrapure water in order to get a final concentration (10 mg mL^{-1}). Then 500 μg of material and 5 μL OVA digestion (1 μg $μL^{-1}$) were mixed in a tube, and a specified volume of ultrapure water was added to make a total volume of 100 μL. After they were incubated for 30 min at 37 °C, 100 μL mixture was centrifuged at 10,000 for 5 min to remove supernatant, and then the deposition was washed with ultrapure water (200 μL) for three times. Finally, 10 μL of eluant (50 % ACN) was used to elute the enriched N-glycans, and the eluate was analyzed by MALDI-TOF-MS. Also, the serum sample was tested to

confirm the enrichment effect of carbonized Mil-101(Cr) for N-linked glycans.

MALDI-TOF-MS analysis

The eluate of glycan sample (1 μL) was deposited on the MALDI plate, and another 1 μL of DHB aqueous solution (10 mg/mL, 0.1 % TFA in 20 % ACN/H_2O solution) was spotted onto the plate as a matrix. MALDI-TOF MS experiments were operated on a 5800 ProteomicsAnalyzer (Applied Biosystems, USA). And the presented procedure is based on procedure of reference [12].

Database search

The detailed structures of N-linked glycans were searched from Glycoworkbench and mass tolerances were 1 Da.

Results and discussion

Synthesis and characterization of carbonized Mil-101(Cr)

The synthetic approach for carbonized Mil-101(Cr) composites was shown in Scheme 1a. The synthesis method included two steps. Firstly, a facile hydrothermal reaction was to get pure Mil-101 crystals, then, after carbonization under high temperature, carbonized Mil-101 composites were obtained.

TEM in Fig. 1 displayed the different morphology of Mil-101(Cr) and carbonized Mil-101. The synthesized Mil-101(Cr) had clear crystal structure (Fig. 1a), which demonstrated that the crystal was synthesized successfully. After high temperature carbonization, the good morphology was replaced by many broken particles (Fig. 1b), it may be that high temperature destroyed its original structure.

Also from field scanning electron microscope (FSEM) (Fig. 2), there was distortion on the particle surface after the carbonization step at 800 °C, but the single particle was clearly visible. Also, the whole structure was loose.

The powder X-ray diffraction patterns (PXRD) were recorded for the structure of Mil-101(Cr) and carbonized Mil-101(Cr) (Fig. S1, ESM). Figure S1a were the PXRD patterns simulated from single crystal structures of Mil-101(Cr), and the experimentally measured XRD patterns for synthesized MOF Mil-101 crystals were displayed in Fig. S1b (ESM). The positions of diffraction peaks of our prepared Mil-101(Cr) crystals (Fig. S1b, ESM) corresponded to the PXRD patterns simulated from single crystal structures of Mil-101(Cr) (Fig. S1a, ESM). The peaks could be seen more clearly from ESM Fig. S1d (in the top right corner), which indicated that the synthesized powder was a typical Mil-101(Cr) structure. After high temperature carbonization (Fig. S1c, ESM), the previous peaks disappeared; characteristic diffraction peaks of at around 24.5, 33.6, 36.2, 41.5, 50.2, 54.8, 63.4, and 65.1 correspond to the specific (012), (104), (110), (113), (024), (116), (214), and (300) planes of Cr_2O_3 lattice.

The nitrogen adsorption–desorption isotherm was used to analyze the specific surface area and porous nature of carbonized Mil-101(Cr). Figure S2a (ESM) showed that the materials have a large BET surface area of 531.88 $m^2\ g^{-1}$. The large surface area was satisfactory for enrichment purposes of glycans. Also, pore size distribution data (Fig. S2b, ESM) displayed that the pore diameter was about 3.03 nm, which displayed a perfect nanopore size to exclude most proteins.

As characterized by Raman spectroscopy (Fig. S3, ESM), two peaks around 1341 cm^{-1} (D-mode) and 1585 cm^{-1} (G-

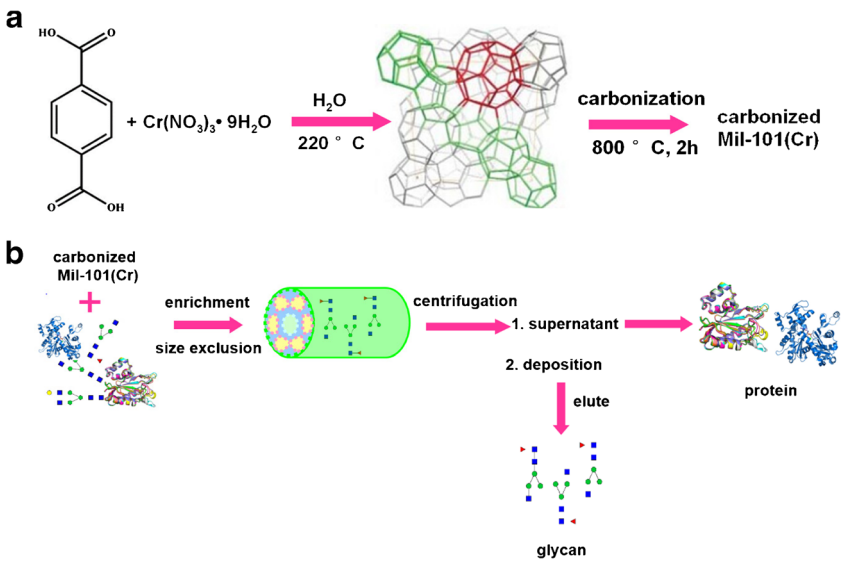

Scheme 1 **a** Synthetic approach for carbonized Mil-101(Cr); **b** selective enrichment of glycans by carbonized Mil-101(Cr)

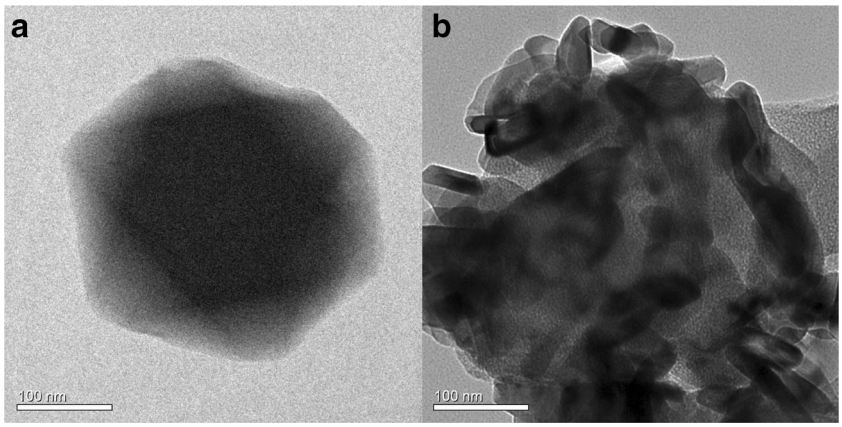

Fig. 1 TEM images of **a** Mil-101(Cr) crystals and **b** carbonized Mil-101(Cr)

mode) were observed, which indicated the existence of carbon in the carbonized Mil-101(Cr) materials [38].

Application of carbonized Mil-101(Cr) in N-linked glycan enrichment

The whole enrichment procedure was shown in Scheme 1b. Figure 3 showed MALDI-TOF MS analysis of N-linked glycans released from OVA. Before enrichment (Fig. 3a), only five glycans could be detected. After enrichment (Fig. 3b), the number of detected glycans increased to 23 and the signal intensity was strongly enhanced. And the glycoforms of the identified glycans from OVA were listed in the Table S1 (ESM). In order to investigate the enrichment ability of glycans, another two materials (Mil-101(Cr) crystals and commercial chromic oxide) were used to enrich glycans as contrast experiments, and the results were shown in Fig. S4a and b, ESM, respectively. There was no clear signal of glycans; we speculated that after calcination, the carbon source provided by the template MOF Mil-101(Cr) had a good distribution in large specific surface, which made the material have great sample loading capability and strong interaction toward glycan molecules. In addition, the MOF enrichment method and the most commonly used glycan enrichment method (graphite affinity column) have been compared. The glycan (from OVA digestion) enrichment efficiency of two methods were displayed Fig. S5 (ESM). It is clearly that our carbonized Mil-101(Cr) materials outperforms graphite affinity column (the enriched numbers of glycans was 23 vs 12). It proved that carbonized Mil-101(Cr) materials can be employed for enriching N-linked glycans with high efficiency.

Moreover, different concentrations of OVA digestion were adopted to investigate the detection limit of the carbonized Mil-101(Cr) (Fig. 4). The glycans with a low concentration (5 ng μL^{-1} of OVA digestion) could be easily detected after enrichment (Fig. 4a). When the concentration of ovalbumin digestion was as low as 2 ng μL^{-1} (Fig. 4b), 13 signals of glycans could still be clearly observed. The above results indicated efficient enrichment of glycans.

Furthermore, the glycoprotein (chicken ovalbumin, 44 kDa, $4 \times 5 \times 7$ nm) and non-glycoprotein (BSA, 66 kDa, $5 \times 7 \times 7$ nm) were selected to evaluate the size-exclusion effect of the carbonized Mil-101(Cr) materials with nanopore structure. We investigated different ratio of ovalbumin digestion/ovalbumin/BSA (Fig. 5 and ESM Fig. S6). When the mass ratio of mixture was up to 1:1500:1500, there was no peak of glycans (Fig. 5a), but the protein peaks were detected before treatment in the linear mode (Fig. 5b). Notably, after enrichment with carbonized Mil-101(Cr) materials, 18 N-linked glycans could be detected clearly without any protein signal (Fig. 5c, d), which displayed the good size-selective enrichment of target glycans, and this attributed

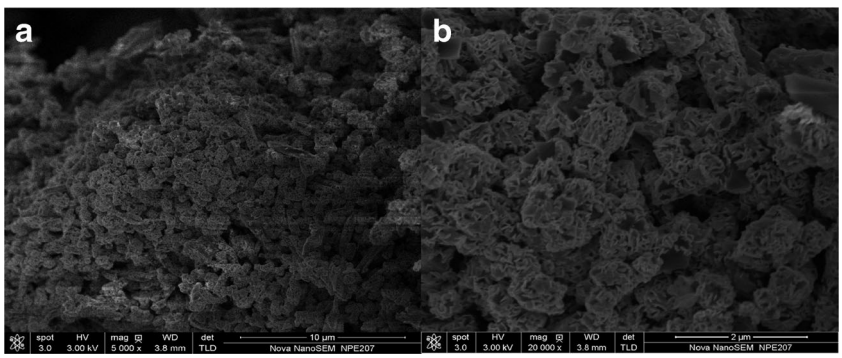

Fig. 2 FSEM images of **a**, **b** carbonized Mil-101(Cr)

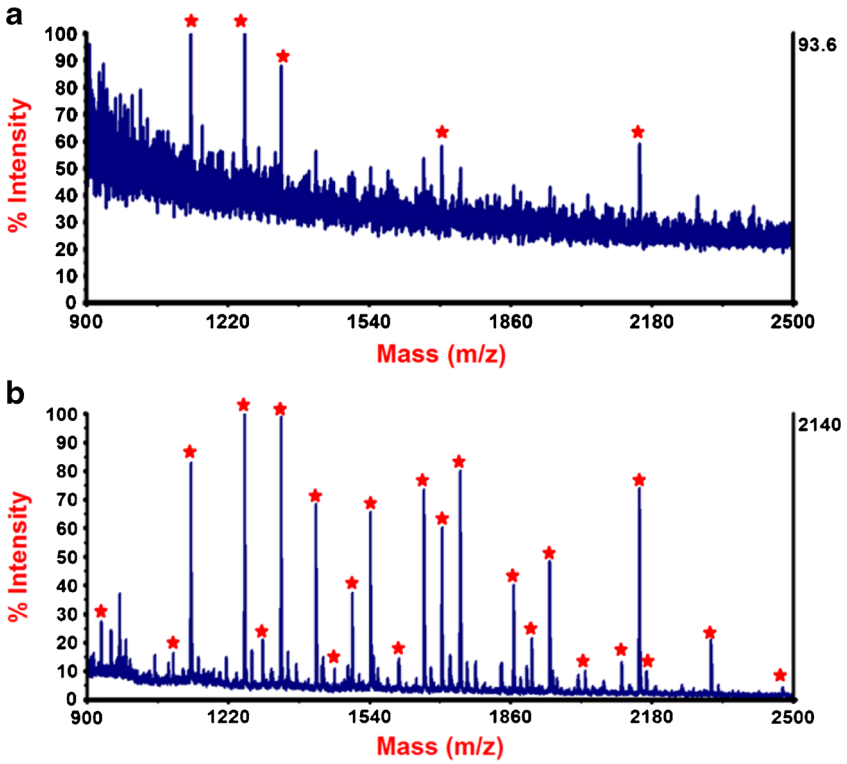

Fig. 3 MALDI-TOF mass spectrum of enriched N-linked glycans from 1 μg μL-1 OVA digests (**a**) before enrichment and (**b**) after enrichment by carbonized Mil-101(Cr), the captured glycans were marked with *red star*

the unique nanopores structure in carbonized materials. Compared with other materials, it had a better size-exclusion effect [35, 39].

The reusability and stability of the carbonized Mil-101(Cr) materials were also tested in this work. The used materials washed by ultrapure water three times were recycled to enrich glycans from OVA digestion. As shown in Fig. S7 (ESM), the result of enrichment in the third time (Fig. S7b) was almost the same as it in the first time (Fig. S7a). As for stability of our materials,

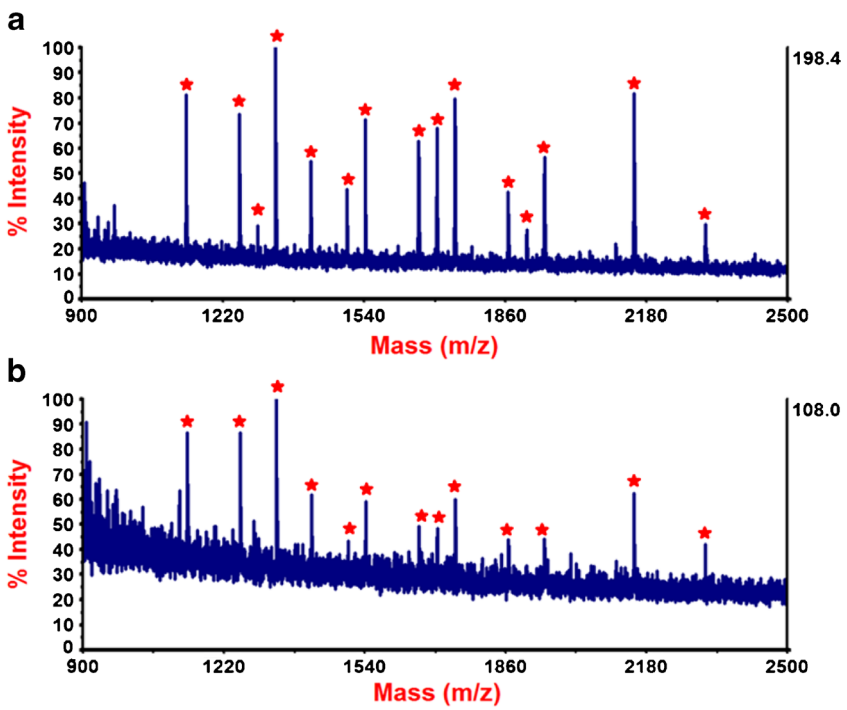

Fig. 4 MALDI-TOF mass spectrum of N-linked glycans enriched by using carbonized Mil-101(Cr) from OVA digests with different concentrations: **a** 5 ng μL^{-1} and **b** 2 ng μL^{-1}

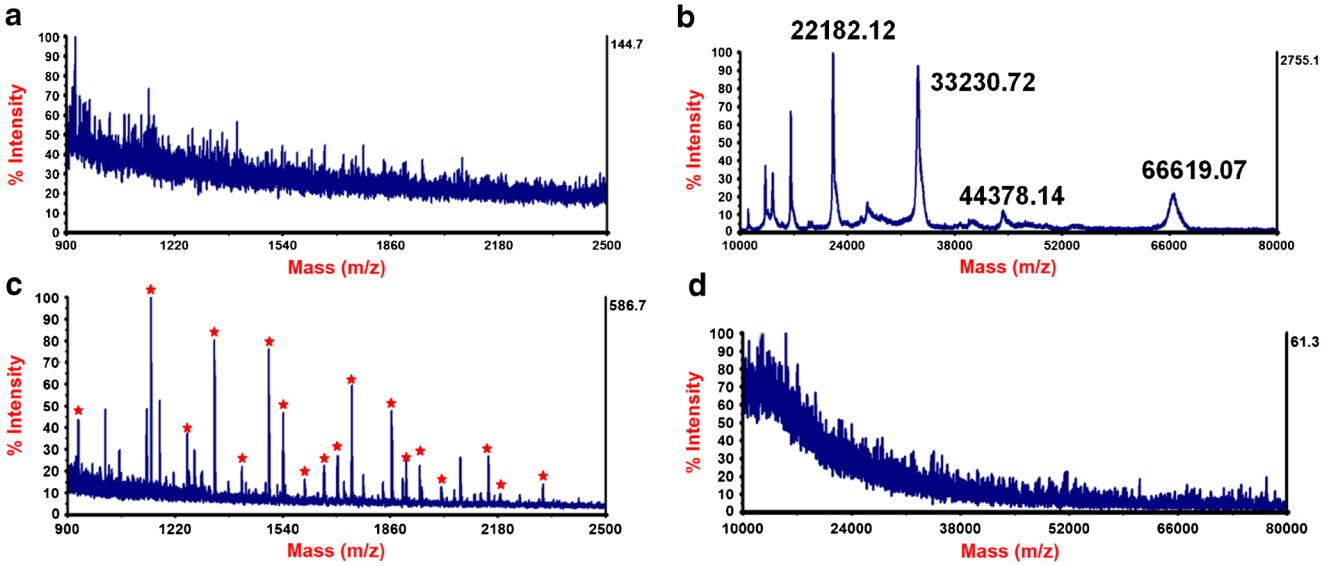

Fig. 5 MALDI-TOF mass spectrum of a mixture of OVA digests, BSA, and OVA. The mass ratio was 1:1500:1500. Supernate before enrichment **a** in positive mode, **b** in linear mode; eluent after enrichment by carbonized Mil-101(Cr) **c** in positive mode, **d** in linear mode

the as-prepared carbonized Mil-101(Cr) was stored at room temperature for 1 month, and then it was used to enrich glycans from OVA again. As shown in the Fig. S8 (ESM), the result of enrichment (Fig. S8b) was similar to the obtained by freshly synthesized material (Fig. S8a). All the results indicated that the carbonized Mil-101(Cr) materials had high enrichment recovery and good stability for the enrichment of N-linked glycans.

Furthermore, we also examined the effectiveness and selectivity of the Mil-101(Cr) materials in practical complex samples. It was applied to capture the glycans from human serum (10 μL) (Fig. 6). After enrichment, 44 glycans can be detected (Fig. 6b). It proved that our material performed a great ability to enrich glycans from a complex sample. The detailed information of enriched glycans from human serum was listed in Table S2 (ESM)

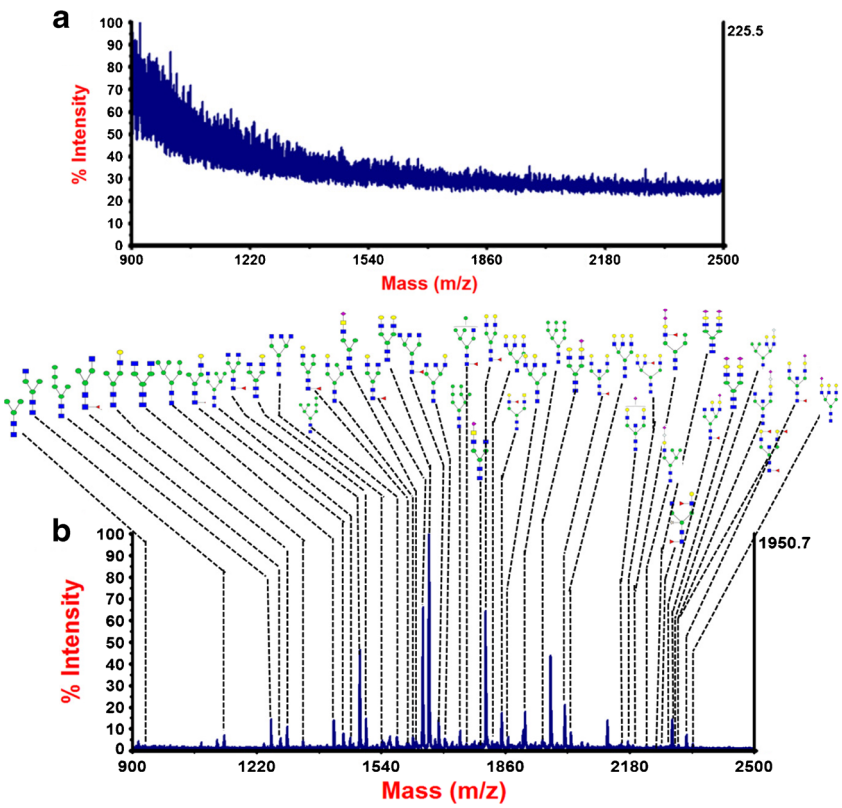

Fig. 6 MALDI-TOF mass spectrum of N-linked glycans in human serum digestion **a** before enrichment; **b** after enrichment by carbonized Mil-101(Cr)

Conclusion

In summary, a novel carbon material with nanopores was prepared by carbonization of MOF Mil-101. Due to the special interaction between abundant carbon and glycan, the suitable nanopore size and high surface area, the material was successfully applied to enrich N-linked glycans. In the enrichment of standard glycoprotein ovalbumin, 23 N-linked glycans could be detected with good repeatability and low limit of detection. Moreover, this material showed a good size-exclusion effect (ovalbumin digestion/ovalbumin/BSA could be to 1:1500:1500). And for complex real human serum, the captured N-linked glycans could be simply detected by MALDI-TOF MS. We can conclude that the glycan enrichment using the carbonized Mil-101(Cr) will have the great potential in the future glycosylation analysis.

Acknowledgments This work was supported by National Basic Research Program of China (Project: 2012CB910604), the National High-Tech R&D Program (Project: 2012AA020202), and the National Natural Science Foundation of China (Project: 21275034 and 21475027).

Authors' contributions All authors have given approval of the final version of the manuscript.

Compliance with ethical standards

Conflict of interest The authors declare that they have no competing interest.

Ethical approval The research followed the tenets of the Declaration of Helsinki, and the use of the human serum samples for research was approved by the Ethics Committee of Zhongshan Hospital, Fudan University. All individual participants gave informed consent for the use of these samples.

References

1. Ohtsubo K, Marth JD. Glycosylation in cellular mechanisms of health and disease. Cell. 2006;126:855–67.
2. Helenius A, Aebi M. Intracellular functions of N-linked glycans. Science. 2001;291:2364–9.
3. Pang PC, Chiu PCN, Lee CL, Chang LY, Panico M, Morris HR, et al. Human sperm binding is mediated by the Sialyl-Lewis^x oligosaccharide on the zona pellucida. Science. 2011;333:1761–4.
4. Wang JX, Wang YN, Gao MX, Zhang XM, Yang PY. Multilayer hydrophilic poly(phenol-formaldehyde resin)-coated magnetic graphene for boronic acid immobilization as a novel matrix for glycoproteome analysis. ACS Appl Mater Interfaces. 2015;7:16011–7.
5. Qin HQ, Zhao L, Li RB, Wu RA, Zou HF. Size-selective enrichment of N-linked glycans using highly ordered mesoporous carbon material and detection by MALDI-TOF MS. Anal Chem. 2011;83:7721–8.
6. Dennis JW, Nabi IR, Demetriou M. Metabolism, cell surface organization, and disease. Cell. 2009;139:1229–41.
7. Zhang W, Wang H, Tang HL, Yang PY. Endoglycosidase-mediated incorporation of ^{18}O into glycans for relative glycan quantitation. Anal Chem. 2011;83:4975–81.
8. Chen SM, LaRoche T, Hamelinck D, Brenner D, Bergsma D, Simeone D, et al. Multiplexed analysis of glycan variation on native proteins captured by antibody microarrays. Nat Methods. 2007;4:437–44.
9. Zhang LJ, Jiang HC, Yao J, Wang YL, Fang CY, Yang PY, et al. Highly specific enrichment of N-linked glycopeptides based on hydrazide functionalized soluble nanopolymers. Chem Commun. 2014;50:1027–9.
10. Budnik BA, Lee RS, Steen JAJ. Global methods for protein glycosylation analysis by mass spectrometry. Biochim Biophys Acta. 1764;2006:1870–80.
11. Block TM, Comunale MA, Lowman M, Steel LF, Romano PR, Fimmel C, et al. Use of targeted glycoproteomics to identify serum glycoproteins that correlate with liver cancer in woodchucks and humans. Proc Natl Acad Sci U S A. 2005;102:779–84.
12. Wang YN, Wang JX, Gao MX, Zhang XM. An ultra hydrophilic dendrimer-modified magnetic graphene with a polydopamine coating for the selective enrichment of glycopeptides. J Mater Chem B. 2015;3:8711–6.
13. Bereman MS, Williams TI, Muddiman DC. Development of a nanoLC LTQ orbitrap mass spectrometric method for profiling glycans derived from plasma from healthy, benign tumor control, and epithelial ovarian cancer patients. Anal Chem. 2009;81:1130–6.
14. Bones J, Mittermayr S, O'Donoghue N, Guttman A, Rudd PM. Ultra performance liquid chromatographic profiling of serum n-glycans for fast and efficient identification of cancer associated alterations in glycosylation. Anal Chem. 2010;82:10208.
15. Selman MHJ, Hemayatkar M, Deelder AM, Wuhrer M. Cotton HILIC SPE microtips for microscale purification and enrichment of glycans and glycopeptides. Anal Chem. 2011;83:2492–249.
16. Ruhaak LR, Miyamoto S, Kelly K, Lebrilla CB. N-glycan profiling of dried blood spots. Anal Chem. 2012;84:396–402.
17. Packer NH, Lawson MA, Jardine DR, Redmond JW. A general approach to desalting oligosaccharides released from glycoproteins. Glycoconj J. 1998;15:737–47.
18. Fan JQ, Kondo A, Kato I, Lee YC. High-performance liquid chromatography of glycopeptides and oligosaccharides on graphitized carbon columns. Anal Biochem. 1994;219:224–9.
19. de Leoz MLA, An HJ, Kronewitter S, Kim J, Beecroft S, Vinall R, et al. Glycomic approach for potential biomarkers on prostate cancer: profiling of N-linked glycans in human sera and pRNS cell lines. Dis Markers. 2008;25:243–58.
20. Li JR, Sculley J, Zhou HC. Metal organic frameworks for separations. Chem Rev. 2012;112:869–932.
21. Jiang JC, Yaghi OM. Brønsted acidity in metal-organic frameworks. Chem Rev. 2015;115:6966–97.
22. Farrusseng D, Aguado S, Pinel C. Metal-organic frameworks: opportunities for catalysis. Angew Chem Int Ed. 2009;48:7502–13.
23. Na K, Choi KM, Yaghi OM, Somorjai GA. Metal nanocrystals embedded in single nanocrystals of MOFs give unusual selectivity as heterogeneous catalysts. Nano Lett. 2014;14:5979–83.
24. Wang C, Liu DM, Lin WB. Metal-organic frameworks as a tunable platform for designing functional molecular materials. J Am Chem Soc. 2013;135:13222–34.
25. Gu ZY, Yang CX, Chang N, Yan XP. Metal organic frameworks for analytical chemistry: from sample collection to chromatographic separation. Acc Chem Res. 2012;45:734–45.
26. Gu ZY, Chen YJ, Jiang JQ, Yan XP. Metal–organic frameworks for efficient enrichment of peptides with simultaneous exclusion of proteins from complex biological samples. Chem Commun. 2011;47:4787–9.
27. Zhao M, Deng CH, Zhang XM, Yang PY. Facile synthesis of magnetic metal organic frameworks for the enrichment of low-

abundance peptides for MALDI-TOF MS analysis. Proteomics. 2013;13:3387–92.
28. Messner CB, Mirza MR, Rainer M, Lutz OMD, Guzel Y, Hofer TS, et al. Selective enrichment of phosphopeptides by a metal–organic framework. Anal Methods. 2013;5:2379–83.
29. Zhao M, Deng CH, Zhang XM. Chem Commun. 2014;50:6228–31.
30. Chen YJ, Xiong ZC. Peng L, Gan YY, Zhao YM, ShenmJ, Qian JH, Zhang LY, Zhang WB. Facile preparation of core−shell magnetic metal−organic framework nanoparticles for the selective capture of phosphopeptides. ACS Appl Mater Interfaces. 2015;7:16338–47.
31. Liu B, Shioyama H, Akita T, Xu Q. Metal-organic framework as a template for porous carbon synthesis. J Am Chem Soc. 2008;130: 5390–1.
32. Banerjee A, Gokhale R, Bhatnagar S, Jog J, Bhardwaj M, Lefez B, et al. MOF derived porous carbon-Fe_3O_4 nanocomposite as a high performance, recyclable environmental superadsorbent. J Mater Chem. 2012;22:9694–19699.
33. Torad NL, Hu M, Kamachi Y, Takai K, Imura M, Naitoa M, et al. Facile synthesis of nanoporous carbons with controlled particle sizes by direct carbonization of monodispersed ZIF-8 crystals. Chem Commun. 2013;49:2521–3.
34. Sun NR, Deng CH, Li Y, Zhang XM. Highly selective enrichment of N-linked glycan by carbon functionalized ordered graphene/ mesoporous silica composites. Anal Chem. 2014;86:2246–50.
35. Zhang QQ, Zhang QH, Xiong ZH, Wan H, Chen XT, Zou HF. Facile preparation of carbon-functionalized ordered magnetic mesoporous silica composites for highly selective enrichment of N-glycans. RSC Adv. 2015;5:68972–80.
36. Cao N, Tan SY, Luo W, Hu K, Cheng GZ. Ternary CoAgPd nanoparticles confined inside the pores of MIL-101 as efficient catalyst for dehydrogenation of formic acid. Catal Lett. 2016;146:518–24.
37. Férey G, Mellot-Draznieks C, Serre C, Millange F, Dutour J, Surble S, et al. A chromium terephthalate-based solid with unusually large pore volumes and surface area. Science. 2005;309:2040–2.
38. Gai S, Yang P, Li C, Wang W, Dai Y, Niu N, et al. Synthesis of magnetic, up-conversion luminescent, and mesoporous core–shell-structured nanocomposites as drug carriers. Adv Funct Mater. 2010;20:1166–72.
39. Sun NR, Zhang XM, Deng CH. Designed synthesis of MOF-derived magnetic nanoporous carbon materials for selective enrichment of glycans for glycomics analysis. Nanoscale. 2015;7:6487–91.